

Grid-based extension method for anchor circle decision using ship-specific characteristics



Gil-Ho Shin¹, Hyun Yang^{2*}

¹ Graduate School of Korea Maritime and Ocean University, Busan, Republic of Korea

² Division of Maritime AI & Cyber Security, Korea Maritime and Ocean University, Busan, Republic of Korea

ARTICLE INFO

Keywords:

Grid-based extension method

Anchor circle

Vessel traffic services (VTS)

Vessel dimensions

Maritime safety

ABSTRACT

With the global increase in maritime cargo volume and vessel size, accurate anchor circle determination is crucial for safe and efficient anchorage management. This study proposes a new grid-based extension method that integrates vessel-specific characteristics with Automatic Identification System (AIS) data to determine anchor circles. Experiments with five vessels at Busan Port demonstrated high accuracy, with a maximum radius error of 9 m, significantly outperforming current Vessel Traffic Service (VTS) systems, which overestimate required radii by 1.7–2.1 times. The method enables immediate field application using existing VTS data, contributing to efficient anchorage management and smart port development.

1. Introduction

The global increase in maritime cargo volume and vessel size, coupled with the trend toward more intelligent, larger, and faster vessels, is driving the growing demand for port anchorage areas while making the maritime navigation environment increasingly complex [1-3]. In this context, Vessel Traffic Service (VTS) plays a crucial role in facilitating port traffic flow and enhancing safety [4].

Maritime safety statistics highlight this challenge, as accidents most frequently occur during navigation and anchorage operations, with a particularly high incidence during bunkering operations while at anchor [5]. This risk is especially important in anchorage areas, an important VTS management zone where multiple vessels must safely coexist for extended periods within limited waters.

As vessels increase in number and size, ensuring safe distances between ships and preventing collisions has become increasingly challenging. The cornerstone of managing this situation safely lies in the accurate determination of anchor circles. An anchor circle is a circular domain indicating the maximum range within which an anchored vessel may swing due to wind pressure and current effects, enabling the maintenance of safe distances between vessels and efficient management of anchorage capacity. In maritime traffic, a ship domain refers to the surrounding waters that must be secured for safe vessel operation, and has become important in restricted waters such as ports and straits. Since [6] first proposed the ship domain concept, it has

* Corresponding author.

E-mail address: yanghyun@kmou.ac.kr

been applied across various maritime safety areas, including collision risk assessment [7, 8], collision avoidance analysis [9, 10], and near-miss detection [11]. Regarding anchored vessel domains, [12] conducted research on anchor chain length and environmental conditions, analyzing anchorage safety during natural disasters.

These ship domains are determined by considering factors such as vessel size, maneuverability, hydrometeorological conditions, and traffic density [13, 14], and can be classified as empirical, knowledge-based, or analytical domains based on the methodology [11]. In this context, an anchor circle can be understood as a specialized domain for anchored vessels.

In maritime safety, grid-based approaches have gained attention for their ability to enable systematic analysis and standardized calculation of spatial information. Recently, [15] and [16] addressed vessel anomaly path detection and maritime environment awareness issues by proposing dynamic grid size adjustment and occupancy grid models, respectively. Additionally, [17] and [18] developed grid-based trajectory prediction models using k-order multivariate Markov chains, while [19] effectively predicted vessel traffic by combining spatiotemporal grid structures with transformer models. Along with these studies, [20] analyzed maritime traffic density in ports by introducing a uniform 60×60 m² grid system.

Despite these important advances in maritime safety research, there are no systematic academic studies of anchor circle determination for anchored vessels. While ship domain concepts for navigating vessels have been researched extensively, scholarly studies focusing on anchor circle determination for anchored vessels are scarce.

This research has three main gaps. First, no academic research has systematically examined individual vessel characteristics in anchor circle determination. In practice, empirical methods are primarily used, while research to systematize and validate these approaches is non-existent. Second, although grid-based approaches have been successfully used in various maritime applications, no research has applied them to anchor circle determination. The potential of grid-based methods to integrate vessel-specific characteristics with spatial calculations remains unexplored. Third, no research has combined Automatic Identification System (AIS) data with the physical characteristics of vessels for anchor circle determination. Specifically, no research has examined anchor circle calculation methods considering the difference between AIS antenna position and the actual anchor drop position.

Against this background, this study proposes a new grid-based anchor circle determination method that integrates vessel physical characteristics with AIS data. To validate this approach, the Busan Port VTS system was analyzed as a case study. Currently, the Busan Port VTS system manages anchorage areas according to operational manuals based on operator experience and expertise. These manuals classify anchorage areas by vessel gross tonnage and stipulate that each anchorage area should manage anchor circles by applying a single fixed radius uniformly to all vessels [21]. Table 1 shows the classification and characteristics of anchorage areas in Busan Port.

Table 1 Classification and Characteristics of Anchorage Areas in Busan Port

Anchorage	Area (km ²)	Allowable Vessel Class (Gross Tonnage)	VTS Standard Radius (m)	Maximum Capacity
N-1	1.13	< 1,000 tons	100	8
N-2	1.77	1,000–2,999 tons	200	7
N-3	6.80	3,000–9,999 tons	300	18
N-4	7.27	10,000–29,999 tons	500	8
N-5	12.02	> 30,000 tons	700	7

Table 1 shows that each anchorage area has a designated range of allowable vessel gross tonnage and applies the same VTS standard radius as an anchor circle radius for all vessels anchoring in that area. These are set at 100, 200, 300, 500, and 700 m for anchorages N-1, N-2, N-3, N-4, and N-5, respectively. Figure 1

shows the operational screen of the current VTS system, showing the anchorage areas and anchor circle management status of anchored vessels in Busan Port.

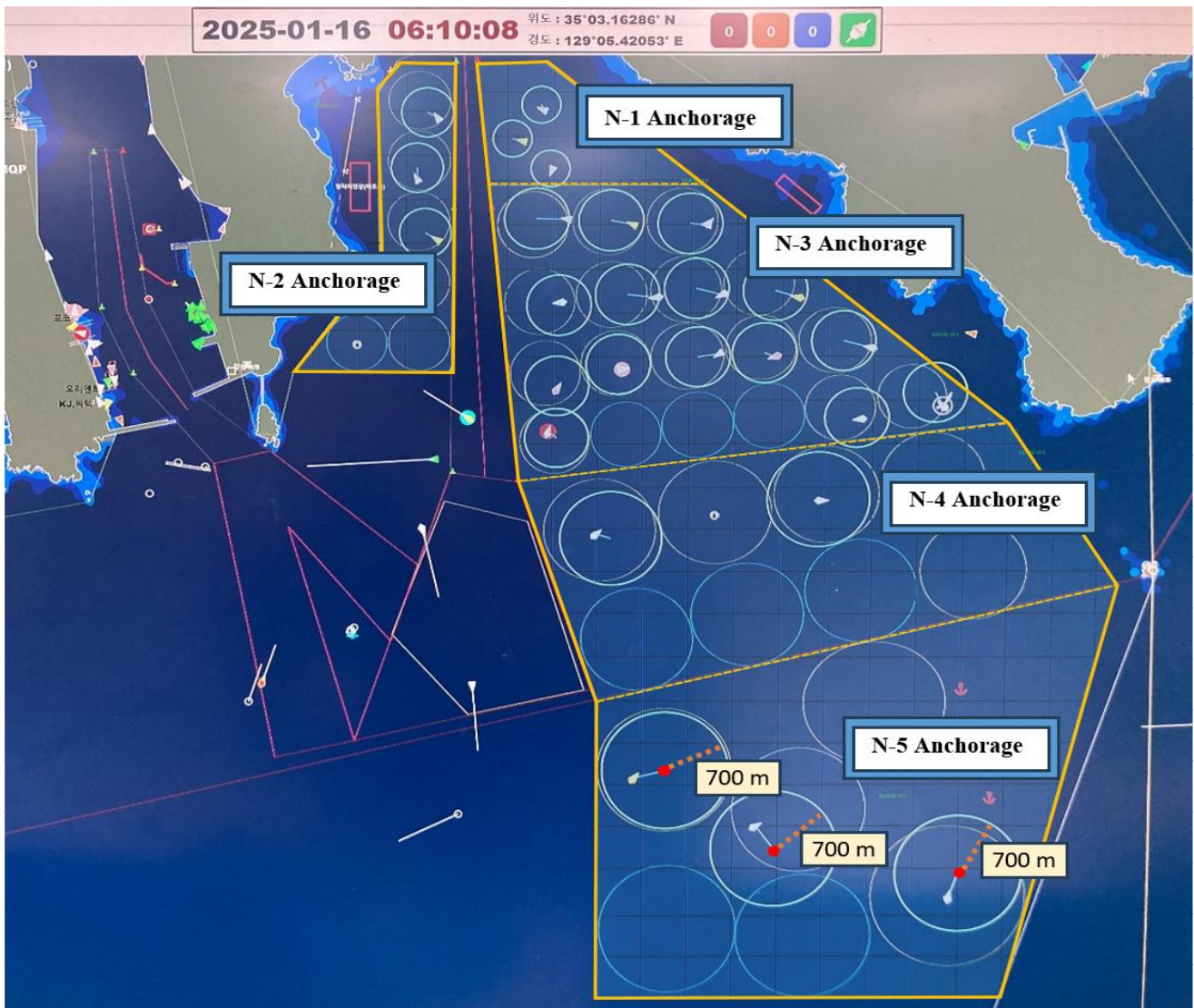


Fig. 1 VTS operating system display showing anchorage areas and anchor circles in Busan

The screen displays information for real-time maritime traffic control, including waterways, vessel positions, movement paths, and anchorage information. Among these elements, the key elements related to anchor circle decision, which is the core subject of this study, are as follows. The yellow solid lines on the screen indicate the total area of anchorages N-1 to N-5, while dotted lines mark the boundaries between anchorage areas. The white circles surrounding the triangular AIS targets of vessels represent the anchor circles uniformly applied to each anchorage area. In anchorage N-5, the center (red dot) of the anchor circle and its radius (orange dotted line, 700 m) are clearly marked.

However, this system has two important limitations. First, the uniform application of a single radius to all vessels by anchorage area, while based on operator experience, fails to reflect individual vessel characteristics. As seen in anchorage N-5 in Figure 1, all anchoring vessels are assigned the same 700-m radius regardless of their gross tonnage or vessel length. Second, when determining the center of the anchor circle, using only the vessel AIS antenna position as a reference creates discrepancies with the actual anchor drop location. This results in inaccurate determination of the vessel's actual movement range, potentially hindering efficient anchorage operation.

To address these issues, this study proposes a new grid-based approach that standardizes and reflects vessel physical characteristics, such as length overall (LOA), AIS antenna position, and anchor chain length in grid units. The key distinguishing features of this study are as follows. First, it presents a standardized framework through a grid-based approach that systematically reflects vessel physical characteristics. This approach overcomes the limitations of individual vessel characteristic non-reflection and the simplified assumptions previously mentioned. Second, it validates the accuracy of the proposed method through comparison with anchor circles derived from actual AIS data. This addresses issues arising from differences between AIS antenna position and actual anchor drop location, enabling customized anchor circle calculation tailored to each vessel's characteristics.

This paper is organized as follows. Section 2 details the grid-based anchor circle calculation method using vessel physical characteristics and AIS data. Section 3 demonstrates the excellence of the proposed method through experiments using actual vessel data from Busan Port anchorage, validating its practicality through comparative analysis with the existing VTS system. Finally, Section 4 presents the study conclusions along with future research directions.

2. Grid-based Extension Methodology Considering Ship Specifications and AIS Antenna Position

Three critical elements must be considered for accurate anchor circle decision: the physical dimensions of the vessel, the actual anchor drop position, and the anchor chain length. Existing maritime traffic management systems have a limitation in comprehensively considering these elements, as they display vessel position only as a single point where the AIS signal originates from the antenna. While our study focuses on vessel movement in port anchorages using geometric factors, it is worth noting that [22] demonstrated how rope damage in mooring systems can reduce dynamic stiffness and potentially expand the movement ranges of structures. This suggests that anchor chain characteristics also act as important variables in movement range prediction, suggesting that future research should incorporate material properties alongside geometric considerations. To address current limitations and develop a more accurate prediction model, this study analyzes the relationship between vessel physical characteristics and AIS data, proposing a grid-based anchor circle decision method that integrates these critical factors.

2.1 AIS Antenna Position and Anchor Drop Position Determination

The AIS equipment on a vessel transmits position information based on the antenna location. The AIS antenna position serves as a crucial reference point when considering the actual vessel dimensions. AIS data provide the distances from the antenna to the bow (d_{bow}) and stern (d_{stern}). The LOA of the vessel can be expressed as the sum of these two distances:

$$LOA = d_{\text{bow}} + d_{\text{stern}} \quad (1)$$

To determine the actual anchor drop position, adjustment is needed considering the distance from the AIS antenna position to the bow. When a vessel anchors in the anchorage area, the actual anchor drop position can be calculated based on the AIS data at the time of anchoring, as reported through very-high-frequency (VHF) communication with VTS:

$$p_{\text{anchor}} = p_{\text{AIS}} + d_{\text{bow}} \cdot v_{\text{heading}} \quad (2)$$

where p_{anchor} is the actual anchor drop position vector (latitude, longitude), p_{AIS} is the AIS antenna position vector (latitude, longitude) at the time of anchoring, and v_{heading} is the heading unit vector.

Figure 2 illustrates the geometric relationship expressed in Equation (2).

As shown in Figure 2, the AIS antenna position (p_{AIS}) is typically on top of a vessel's bridge, while the actual anchor drop position (p_{anchor}) is at the foremost point of the bow, where the anchor is deployed.

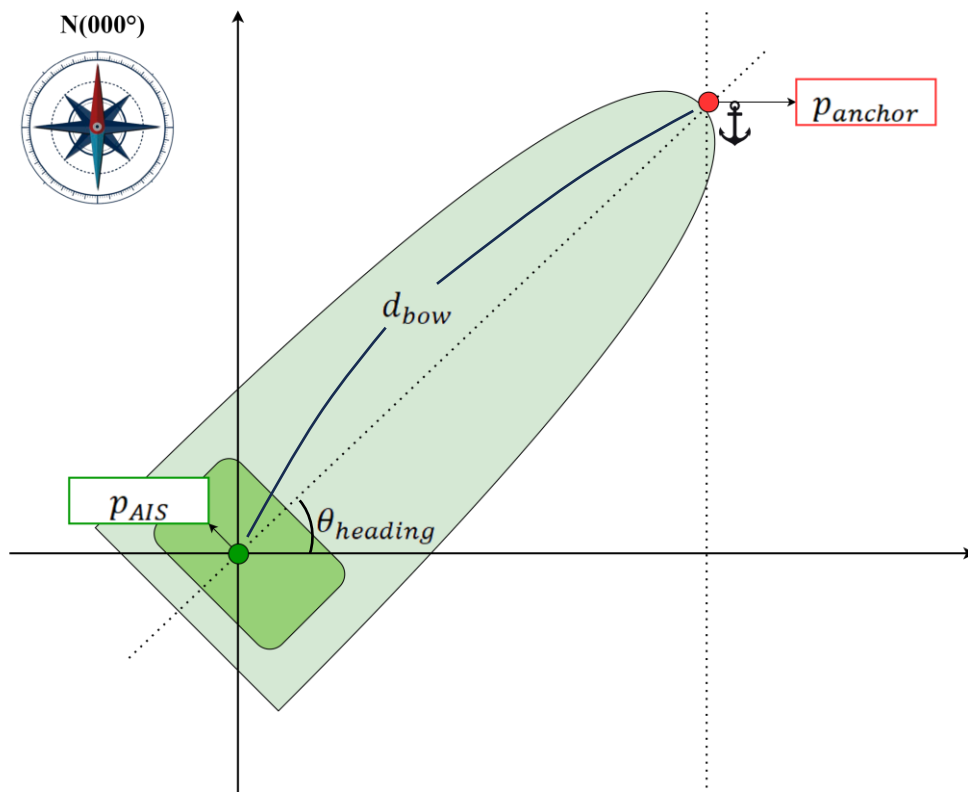


Fig. 2 Determination of the anchor drop position using AIS antenna location and heading direction vector

The vector from p_{AIS} to p_{anchor} has magnitude d_{bow} and a direction determined by the vessel's heading angle ($\theta_{heading}$), defined as the angle increasing clockwise with north as the reference (000°), as illustrated by the compass in Figure 2 using the value provided in the AIS data. The heading unit vector $v_{heading}$ is calculated using $\theta_{heading}$:

$$v_{heading} = (\cos \theta_{heading}, \sin \theta_{heading}) \quad (3)$$

This accurate calculation of the anchor drop position serves as the reference point for determining the anchor circle and is consistently used in the subsequent grid-based method and actual vessel movement range analysis. When an anchored vessel rotates, the trajectories drawn by the bow and stern around the antenna position have different radii, making accurate reflection of these physical characteristics essential for safe anchorage management.

2.2 Algorithmic Approaches

The anchor chain length is important for determining the anchor circle radius. The length of the anchor chain directly determines the range within which a vessel can rotate while anchored, forming the basic radius of the anchor circle. The length of the anchor chains used on vessels is typically expressed in units of shackles. One shackle equals 15 fathoms, which can be converted to meters as follows:

$$1 \text{ shackle} = 15 \times 6 \text{ feet} = 90 \text{ feet} \approx 27.432 \text{ m} \quad (4)$$

In Equation (4), 6 is the number of feet in 1 fathom. Therefore, the actual anchor chain length is calculated according to the number of shackles deployed, as reported to the VTS:

$$L_{chain} = N_{shackle} \times 27.432 \quad (5)$$

where L_{chain} is the total length of the anchor chain (m), and $N_{shackle}$ is the number of shackles deployed as reported to the VTS.

The anchor chain length calculated by this method is the foundation for the grid extension calculations discussed below and is important in the final determination of the anchor circle radius.

2.3 Grid-based Extension for Anchor Circle Radius Calculation

To determine the anchor circle of a vessel, the maximum space that the vessel may occupy while anchored is calculated using a grid-based approach. This approach was selected after careful consideration of the specific requirements for anchor circle determination.

The grid-based approach has several distinct advantages. First, it enables standardized quantification of spatial relationships, allowing precise integration of vessel-specific physical attributes with AIS data. Second, it provides a flexible framework that can accommodate variation in vessel dimensions while maintaining computational efficiency. Third, the discretization of continuous space into grid units facilitates practical implementation in maritime traffic control systems and allows for consistent visual representation across different scales.

This study sets each grid to 10 m to calculate the physical dimensions of a vessel and movement range in grid-based units. Previous coastal spatial modeling studies have employed grid-based approaches for maritime spatial analysis, with spatial resolutions typically ranging from approximately 3 to 10 m to achieve an optimal balance between terrain representation accuracy and computational efficiency [23, 24]. Accordingly, this specific grid size was selected to balance computational efficiency with the spatial precision required for effective anchorage management, considering the typical dimensions of vessels and the resolution capabilities of modern VTS systems. This 10-m resolution aligns with established practices in maritime spatial modeling while providing sufficient granularity for accurate vessel movement analysis.

The anchor circle calculation using grid-based extension considers the following elements sequentially. First, the center point of the anchor circle incorporates the actual anchor drop position (p_{anchor}) calculated from Equation (2). Then, it calculates the basic radius within which the vessel can rotate, considering the anchor chain length (L_{chain}) derived from Equation (5). Finally, it determines the final radius by adding the distance from the antenna to the stern (d_{stern}) to account for the total vessel length. The final radius of the anchor circle is calculated as:

$$R_{\text{decision}} = d_{\text{stern}} + d_{\text{bow}} + L_{\text{chain}} \quad (6)$$

where R_{decision} is the decided-upon anchor circle radius (m). Given the anchor circle radius, the conversion to the number of grids is expressed as:

$$N = \left\lceil \frac{R}{G_{\text{side}}} \right\rceil, R \in \{R_{\text{decision}}, R_{\text{actual}}\} \quad (7)$$

where N is the number of grids corresponding to the radius, R is the anchor circle radius (m), which can be either the decided-upon (R_{decision}) or actual (R_{actual}) radius, and G_{side} is the grid size (10 m). Notably, the direction of grid extension does not affect the calculation results because an anchor circle is defined solely by its maximum radius from the center point. However, grid extension should maintain a consistent direction for consistent results.

The significance of this approach lies in its practical applications. By enabling more accurate determination of anchor circles tailored to individual vessel characteristics, the grid-based method optimizes anchorage space utilization while maintaining safety margins. Furthermore, the ability of the approach to be implemented using existing AIS data infrastructures enhances its feasibility for immediate adoption in operational VTS environments, making it valuable for busy ports where efficient use of limited anchorage space is critical.

2.4 Actual Anchor Circle Decision Method

To determine the actual anchoring range of a vessel accurately, it is necessary to determine actual anchor circles based on AIS data. This section explains the method for determining actual anchor circles to validate the accuracy of the proposed grid extension-based anchor circle decision method.

To calculate the actual radius of the anchor circle, both the actual anchoring position and the extreme point of the vessel must be determined. The actual anchoring position uses the anchor drop position (p_{anchor}) calculated from Equation (2). The extreme point of the vessel must be calculated by incorporating the distance to the stern from the antenna position, as AIS data provide only the antenna position. Figure 3 illustrates the geometric relationship for calculating the extreme point at each time step.

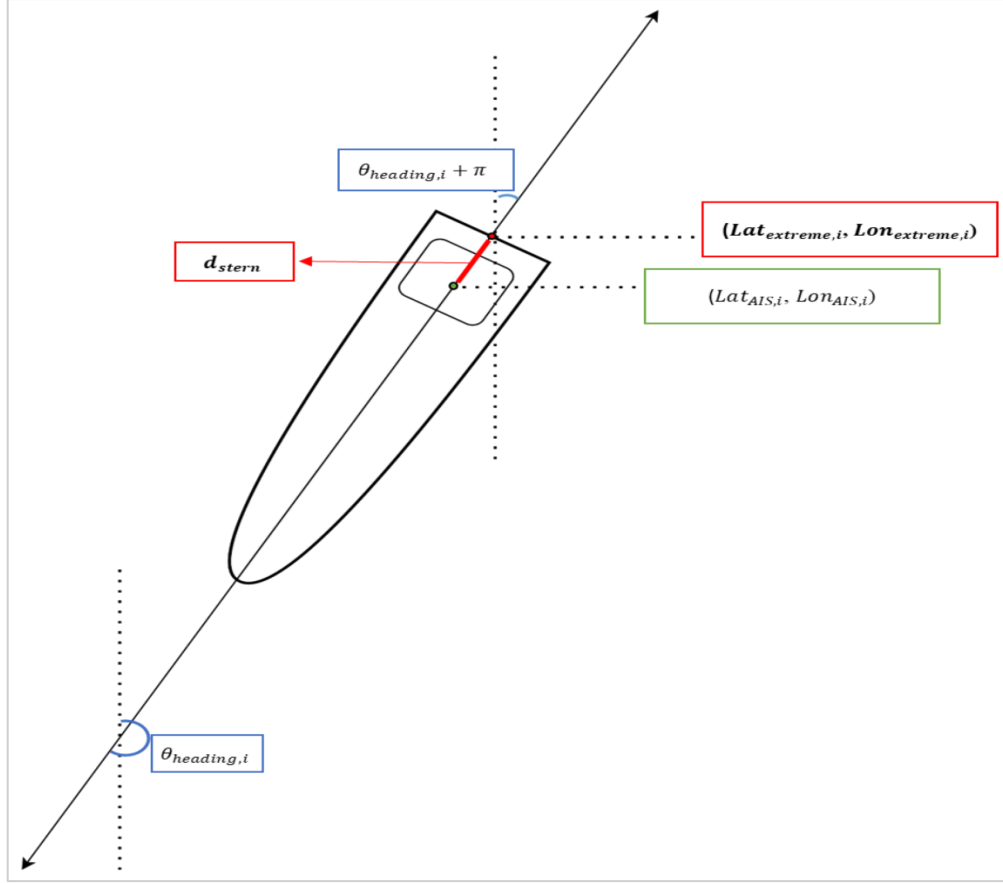


Fig. 3 Spatial configuration of AIS position and stern extreme point for determination of the actual anchor circle radius

Here, the green point is the AIS antenna position ($Lat_{AIS,i}, Lon_{AIS,i}$) at time step i , while the red point is the extreme point ($Lat_{\text{extreme},i}, Lon_{\text{extreme},i}$) at that time step. The red line connecting these two points equals the physical distance from the antenna to the stern, d_{stern} . The extreme point is located at a distance of d_{stern} in the direction rotated 180° (π rad) from the heading direction ($\theta_{\text{heading},i}$) based on the AIS antenna position. This geometric relationship forms the basis for the following equations:

$$Lat_{\text{extreme},i} = Lat_{AIS,i} + d_{\text{stern}} \cdot \cos(\theta_{\text{heading},i} + \pi) \quad (8a)$$

$$Lon_{\text{extreme},i} = Lon_{AIS,i} + d_{\text{stern}} \cdot \sin(\theta_{\text{heading},i} + \pi) \quad (8b)$$

where π is 180° (π rad) for converting from bow direction to stern direction.

The extreme point is determined based on the following criteria. First, as a limit on the distance increase, the position is selected at the point where the distance from the center no longer increases in the AIS data. Then, continuous data over a certain period are analyzed to eliminate the effects of temporary anomalies or noise.

Using these determined extreme points, the actual anchor circle radius is calculated as follows:

$$R_{\text{actual}} = \max_i \sqrt{(Lat_{\text{extreme},i} - Lat_{\text{anchor}})^2 + (Lon_{\text{extreme},i} - Lon_{\text{anchor}})^2} \quad (9)$$

where R_{actual} is the actual anchor circle radius, Lat_{anchor} and Lon_{anchor} are the latitude and longitude of the actual anchor drop position calculated from Equation (2), i is the time index of AIS data, and \max_i is the maximum value operator over time i .

The actual anchor circle calculated with this method serves as an objective standard for evaluating the accuracy of the proposed grid extension-based anchor circle decision method. Section 3 validates the effectiveness of this method through experiments applying it to actual vessel data.

2.5 Performance Evaluation Metrics

This section explains the performance metrics for quantitatively evaluating the accuracy of the proposed grid extension-based anchor circle decision method. Two main aspects of the performance are evaluated based on comparisons of anchor circle radii and grid numbers.

The first evaluation metric is the radius error (RE), which is the difference between the radius calculated from Equation (6) and the actual radius derived from Equation (9), expressed as:

$$RE = |R_{\text{decision}} - R_{\text{actual}}| \quad (10)$$

The second evaluation metric is the grid number error (GNE), which is the difference in the number of grids after converting each radius through Equation (7):

$$GNE = |N_{\text{decision}} - N_{\text{actual}}| \quad (11)$$

where N_{decision} is the number of grids converted from the decided radius (R_{decision}), and N_{actual} is the number of grids converted from the actual radius (R_{actual}).

RE and GNE evaluate the accuracy of anchor circle determination from different perspectives. RE calculates the physical error in m, directly quantifying the precision between the predicted anchor circle radius and actual radius. GNE has two important advantages by converting continuous RE values into discrete grids of 10-m units. First, gridification enhances computational efficiency, facilitating real-time processing. Second, by rounding up m-based errors to grid units, safety margins are automatically incorporated, enabling more conservative safety-centered anchor circle decisions.

Using these two evaluation metrics, the accuracy of the proposed methodology can be analyzed. The RE evaluates accuracy in m compared to the actual movement range, while the GNE evaluates accuracy from an implementation perspective. Section 3 analyzes the experimental results based on these evaluation metrics and validates the effectiveness of the proposed methodology.

3. Experiment and Results Analysis

This section systematically analyzes the experimental results to validate the effectiveness of the grid-based anchor circle decision method proposed in Section 2. This quantitatively evaluates how our method, which considers vessel physical characteristics and actual operational environments, is an improvement over the existing position-based approach.

The experiment has three core objectives. First, it validates how accurately the proposed grid extension method determines the actual movement range of the vessel. Second, it analyzes how vessel physical characteristics (including LOA, AIS antenna position, and anchor chain length) influence anchor circle decisions. Third, it evaluates the generalization potential of the method through experiments with vessels of various types and sizes conducted using actual vessel data from the Busan Port anchorage, selecting periods of favorable weather and stable anchoring states to ensure data reliability. The experimental results were analyzed based on the performance evaluation metrics presented in Section 2.5, objectively validating the accuracy and practicality of the proposed methodology.

3.1 Data Collection and Preprocessing

Data collected for this experiment targeted vessels anchored in Busan Port using a systematic collection and preprocessing approach to ensure data reliability and accuracy, thereby guaranteeing the objectivity of the results.

This study used AIS data as the primary data source. As noted by [25], AIS is a system with potential for intelligent analysis that can replace or complement manual surveillance at sea. International commercial vessels above certain tonnage are required to be equipped with AIS, including cargo ships, passenger vessels, and tankers. AIS broadcasts both dynamic and static vessel information through standardized VHF transceivers [26].

The dynamic information includes vessel position, speed, course, heading angle, rate of turn, destination, and estimated time of arrival, while the static information includes vessel name, MMSI ID, message ID, vessel type, vessel dimensions, and current time. Vessels in navigation transmit this information at 2–10-second intervals, while anchored vessels transmit at 3-minute intervals, receiving the same information from other vessels within 20 nautical miles. This rich AIS data provides essential baseline information for anchor circle analysis. For systematic AIS data collection, this study used two core systems operated by the Ministry of Oceans and Fisheries. The Port Management Information System (Port-MIS) provides basic vessel information and anchoring records, while the General Information Center on Maritime Safety and Security (GICOMS) provides detailed AIS data for each vessel. The collection period was from 3 to 6 June 2023.

The collected AIS data include both dynamic and static vessel information. The dynamic information includes vessel position information (latitude, longitude) and heading angle, while the static information includes the physical distances from the AIS antenna to the bow (d_{bow}), stern (d_{stern}), port side (d_{port}), and starboard side ($d_{\text{starboard}}$). For use in anchor circle calculation, this study defines d_{bow} as d_{bow} and d_{stern} as d_{stern} . Strict criteria were applied in data selection to enhance reliability. To minimize weather-related effects, only data from periods with wind speeds below 14 m/s and wave heights below 3 m were selected, referencing the Korea Meteorological Administration's strong wind advisory criteria [27].

Only data from vessels in normal anchoring states without anchor chain loss or dragging were selected for analysis, and only vessels with continuous AIS signal availability were included to ensure data quality. Applying these criteria, five vessels were ultimately selected for analysis. These vessels were specifically chosen from anchorages N-4 and N-5, which accommodate vessels exceeding 10,000 tons (Table 1). This selection focuses on larger vessels that require more careful management due to their potential to cause greater environmental and human casualties in case of maritime accidents. Table 2 summarizes the main parameters of the selected vessels.

Table 2 Specifications and Initial Parameters of Sample Vessels for Anchor Circle Analysis

MMSI	Width	d_{bow}	d_{stern}	L_{chain}	θ_{heading}	p_{anchor}
215077***	36	194	38	8	202	35.020249°N, 129.065102°E
255806***	32	167	23	5	291	35.026097°N, 129.073921°E
373579***	28	157	18	5	1	35.043717°N, 129.074633°E
636014***	32	230	56	5	314	35.023437°N, 129.049683°E
636022***	32	201	28	6	94	35.006826°N, 129.051647°E

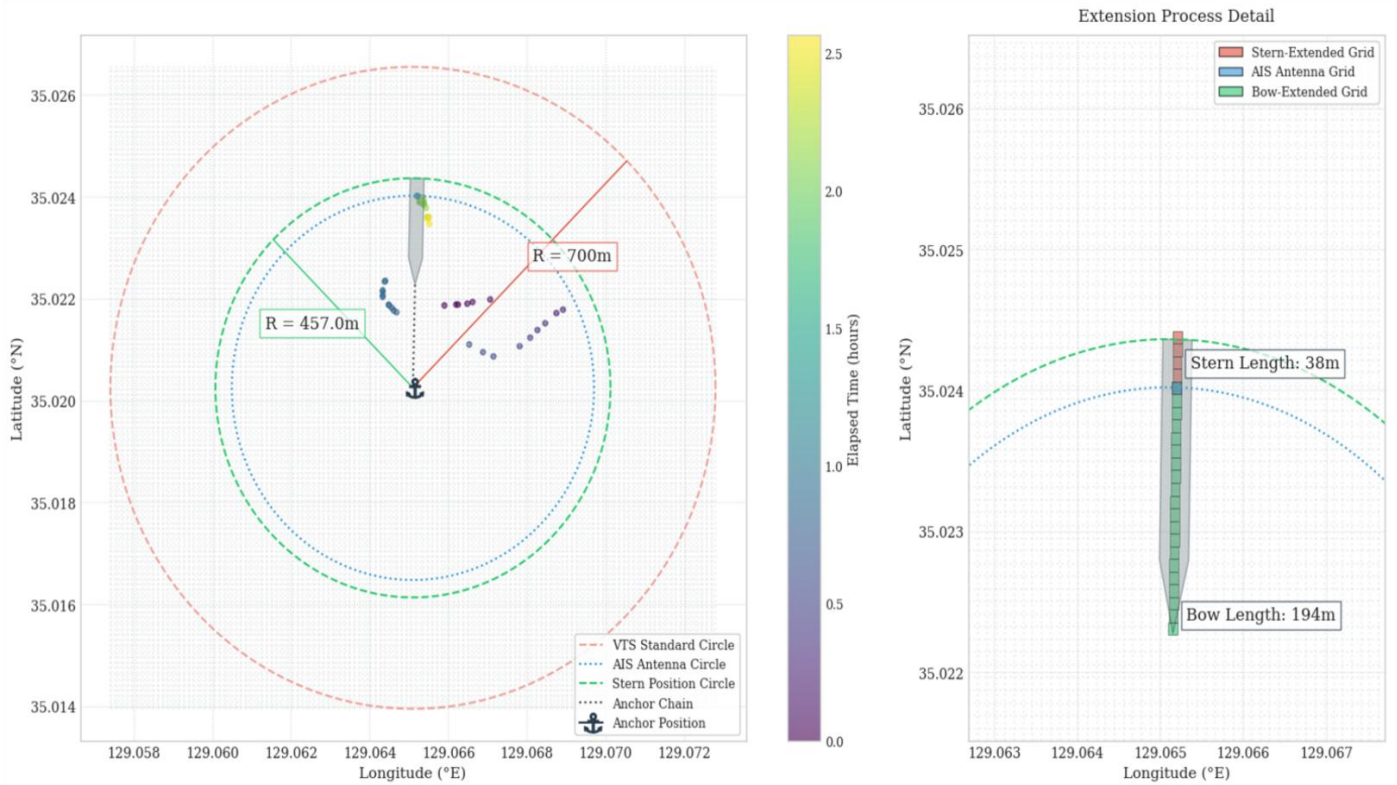
Table 2 includes the width, distance from antenna to bow (d_{bow}), distance to stern (d_{stern}), anchor chain length (L_{chain}), heading angle at time of anchoring (θ_{heading}), and actual anchor drop position (p_{anchor}) for each vessel. These parameters were used as baseline data for applying the grid-based anchor circle decision method proposed in Section 2.

3.2 Comparative Analysis of Decided-upon and Actual Anchor Circles

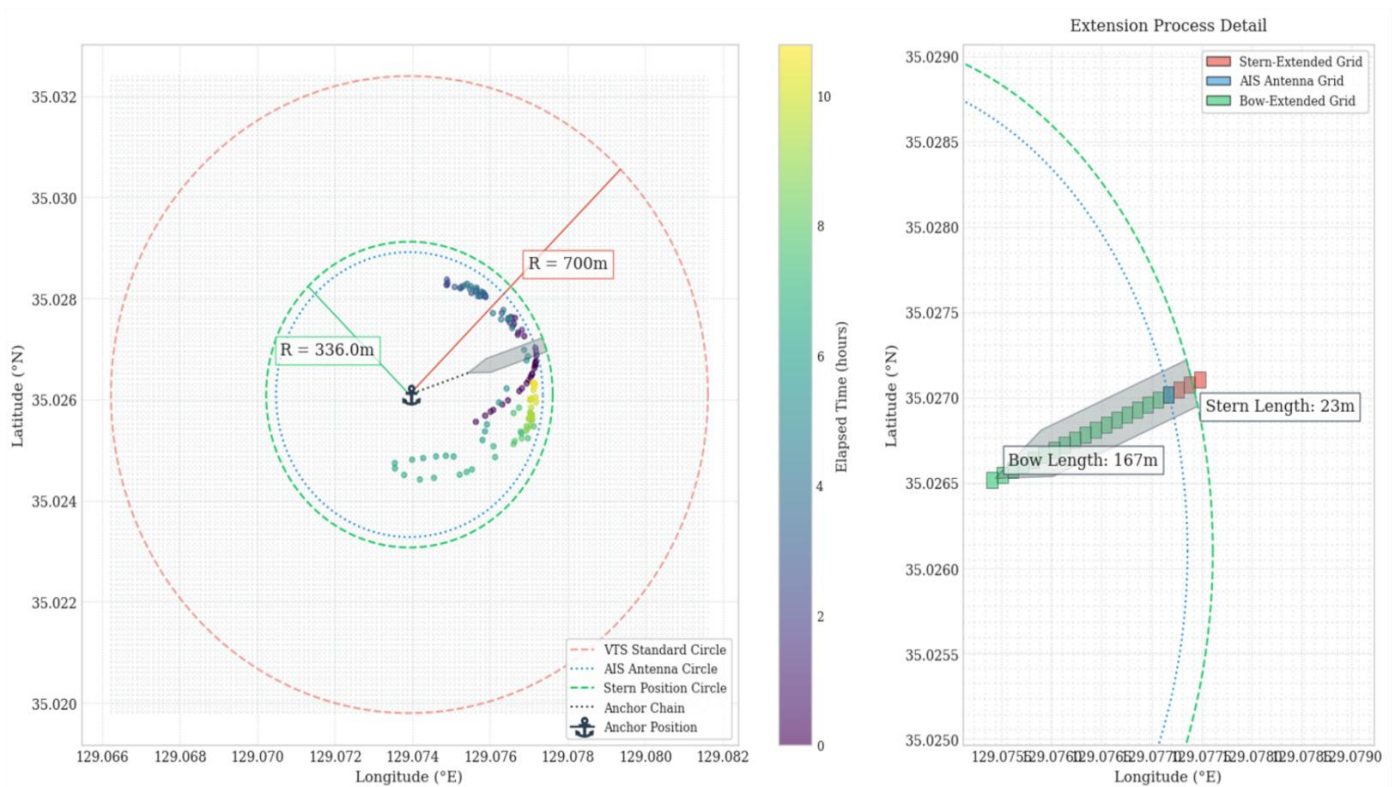
This section validates the accuracy of the grid-based anchor circle decision method proposed in Section 2. We quantitatively compare the determined anchor circles with actual anchor circles derived from AIS data,

and demonstrate the differences from the fixed radius approach of the existing VTS system. All numerical values are rounded to the nearest decimal place.

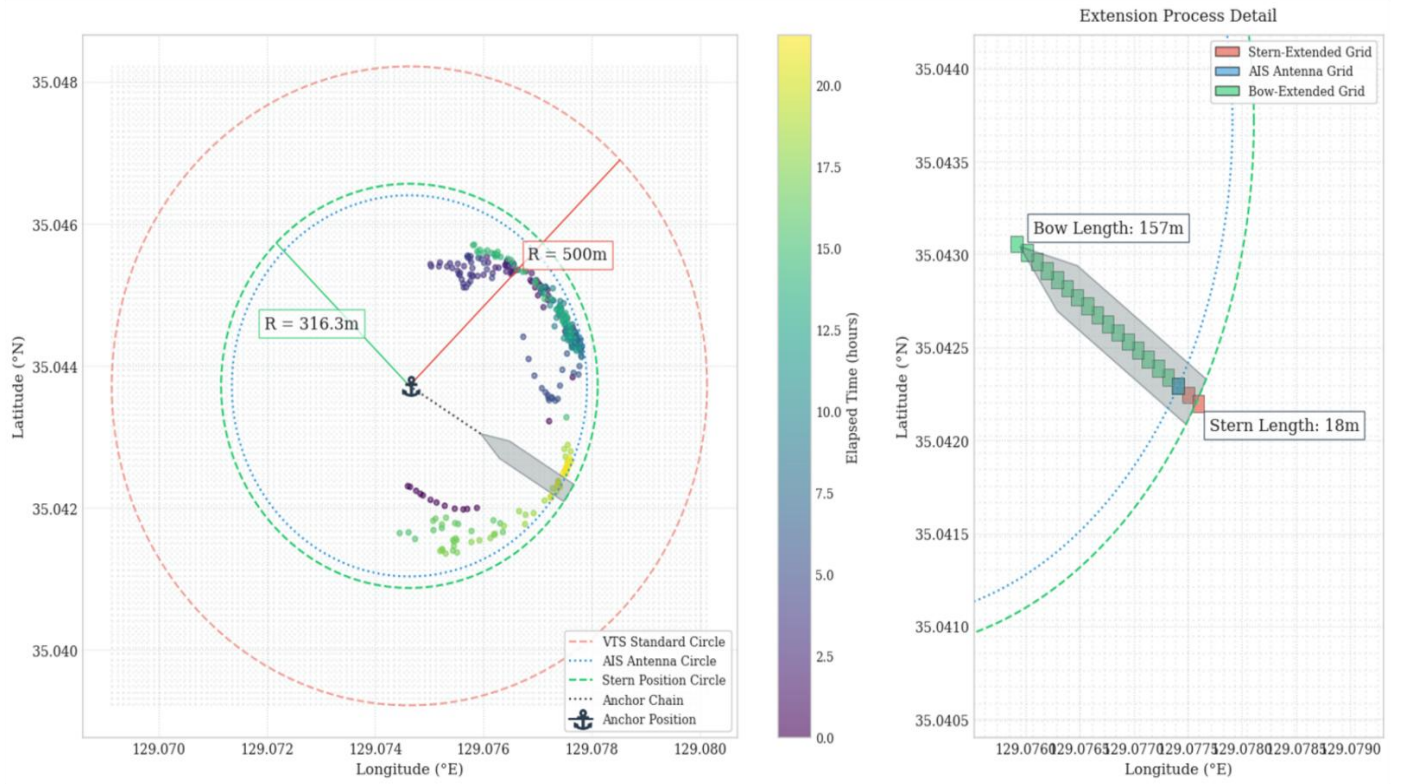
To validate accuracy, we first analyzed the actual movement characteristics of vessels. Based on AIS data from the five vessels under study, we calculated their actual movement ranges and visualized them as in Figure 4, which shows the grid extension-based anchor circle analysis results for each vessel, labeled (a)–(e).



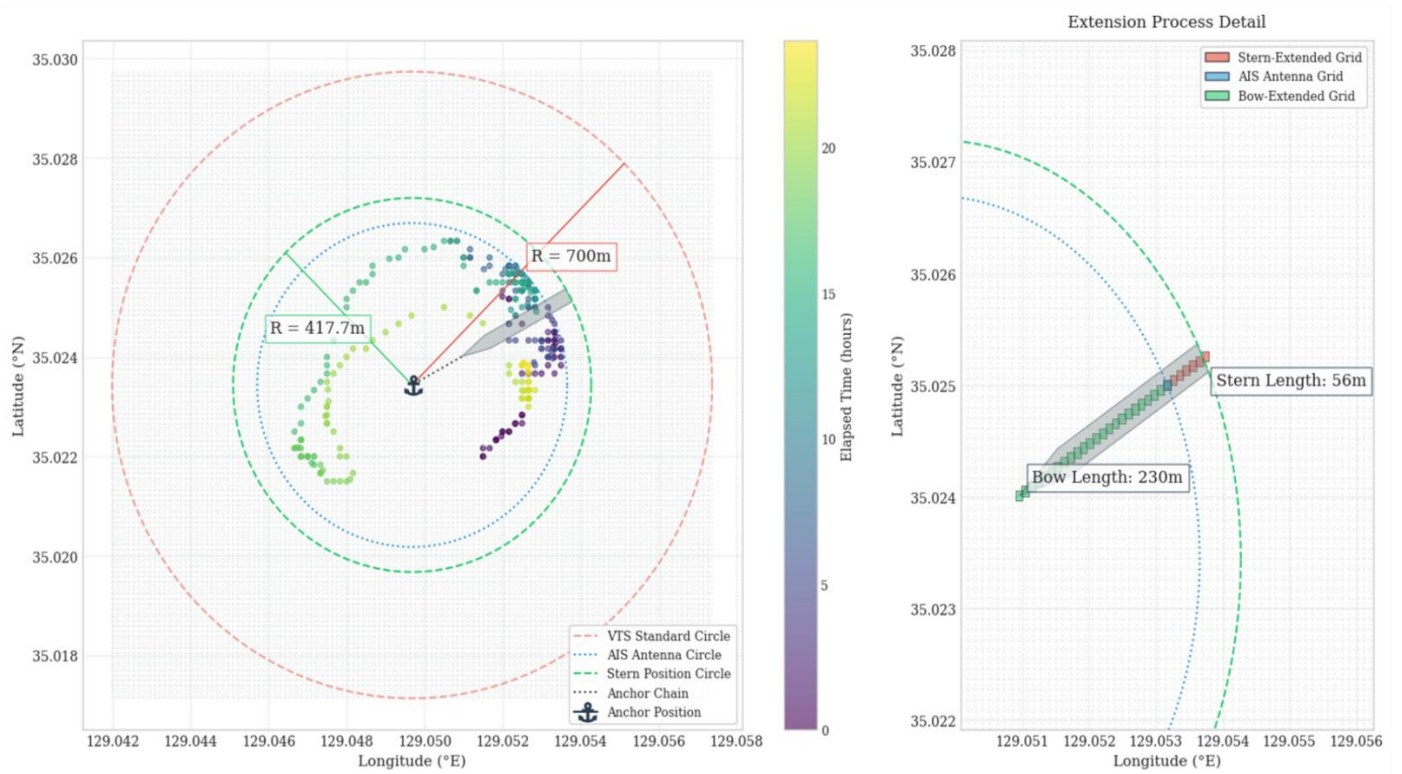
(a) MMSI 215077***



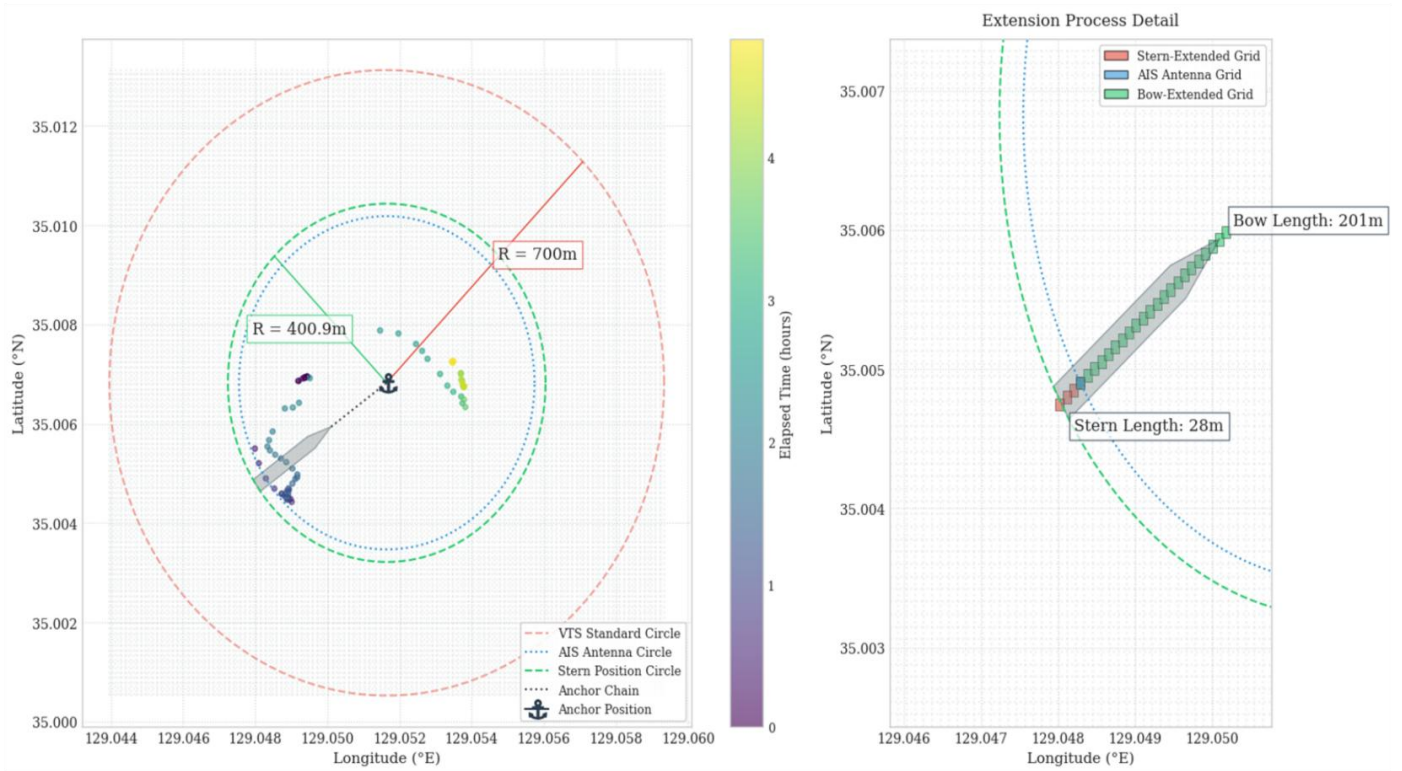
(b) MMSI 255806***



(c) MMSI 373579***



(d) MMSI 636014***



(e) MMSI 636022***

Fig. 4 Visualization of Ship Anchor Circle Analysis with Grid-based Extension Method: Comparison of Movement Ranges with VTS Standard Radius (N-4: 500 m, N-5: 700 m)

The left side of each figure shows the overall anchor circle and vessel trajectory, while the right side shows a detailed view of the grid-based extension process. The actual vessel movement over time is represented by a gradient changing from purple to yellow, with the color bar indicating the elapsed time in hours from the time of anchoring. The red dotted circles are the standard radius used in the existing VTS system for each anchorage area: 700 m for vessels (a), (b), (d), and (e) anchored in N-5, and 500 m for vessel (c) anchored in N-4 (refer to Table 1).

For (a), the VTS standard radius of 700 m for anchorage N-5 was approximately 1.7 times the actual anchor circle radius of 457 m (Figure 4(a)). Similarly, Figure 4(b) shows that for (b) in anchorage N-5, the VTS standard radius of 700 m was about 2.1 times larger than the actual anchor circle radius of 336 m. In Figure 4(c), (c) in anchorage N-4 with a VTS standard radius of 500 m, as specified in Table 1, was 1.8 times the actual anchor circle radius of 316 m. In Figure 4(d), despite being the largest vessel anchored in N-5, (d) had an actual anchor circle radius of only 418 m, a 1.7-times difference from the VTS standard radius of 700 m. Figure 4(e) also showed that the VTS standard radius of 700 m was 1.7 times larger than the actual anchor circle radius of 401 m for (e) in anchorage N-5. These results demonstrate that the fixed radius approach of the current VTS system overestimates actual required vessel ranges. To address this issue, we quantitatively validated the accuracy of the proposed grid-based anchor circle decision method. Table 3 compares the determined and actual anchor circles for each vessel.

Table 3 Comparative Analysis of the Determined and Actual Anchor Circles

MMSI	$R_{decision}(m)$	$N_{decision}$	$R_{actual}(m)$	N_{actual}	RE (m)	GNE
215077***	451	46	457	46	6	0
255806***	327	33	336	34	9	1
373579***	312	32	316	32	4	0
636014***	423	43	418	42	5	1
636022***	394	40	401	41	7	1

Analysis of Table 3 reveals minimal differences between the decided-upon and actual anchor circle radii. For the vessel in Figure 4(a), the difference between the radius of 451 m calculated by Equation (6) and the actual radius of 457 m derived from Equation (9) was merely 6 m. The vessel in Figure 4(b) had a larger RE of 9 m; however, when converted to grids according to Equation (7), this difference amounted to a single grid. The vessel in Figure 4(c), in anchorage N-4, had the smallest RE of 4 m, validating the excellence of the proposed method. The largest vessel, shown in Figure 4(d), had a small RE of 5 m, proving that stable decisions are possible regardless of vessel size. The vessel in Figure 4(e) had an RE of 7 m and a GNE of 1.

These results demonstrate that the RE calculated by Equation (10) ranges from 4 to 9 m, and the GNE calculated by Equation (11) is 1 at most, proving that the proposed method provides sufficient accuracy in actual maritime traffic control environments. Particularly when compared to the 1.7–2.1 times overestimation of the VTS fixed radius approach, the proposed method demonstrates its ability to determine actual required vessel ranges with remarkable accuracy.

As a result, VTS operators and vessel masters can utilize the recovered anchorage space more efficiently and manage collision risks more effectively. Under the current VTS practice, vessels often wait outside the anchorage until space becomes available, which prolongs their anchoring wait time. Reducing overestimation allows more ships to berth promptly and enables earlier detection of anchor dragging or other anomalies, enhancing accident prevention.

Although our study focuses on geometric and AIS-based estimation, the importance of precise prediction is discussed in other domains. For example, [28, 29] examined the mechanical behavior and residual strengths of aramid HMPE and polyester mooring ropes under various conditions, including bedding-in loading history and artificial damage. Although these studies focus on material-level performance, they provide valuable insights into the broader challenges of minimizing uncertainties in anchoring systems and emphasize the importance of precise anchor positioning.

4. Discussion

The experimental results of the grid-based anchor circle decision method proposed here have significant performance differences from the existing VTS system. The most notable finding is that the fixed-radius approach used by the current Busan Port VTS system substantially overestimates the required radius. According to the experimental results, for vessels in anchorage N-5 (Figure 4(a), (b), (d), (e)), the VTS standard radius of 700 m was 1.7–2.1 times larger than the actual anchor circle radius (336–457 m), while for the vessel in anchorage N-4 (Figure 4(c)), the VTS standard radius of 500 m was approximately 1.8 times larger than the actual radius of 316 m.

These results suggest that the current anchor circle decision method of the VTS system, which is based on empirical methodology, requires reconsideration. As shown in Figure 4, the difference between the VTS standard radius (red dotted circle) and actual vessel movement range (trajectory indicated by color gradation) is large, indicating inefficient utilization of anchorage space.

The performance evaluation metrics of the proposed grid-based method quantitatively demonstrate its accuracy. As seen in Table 3, the RE for the five vessels ranged from 4 to 9 m, and the GNE was 1 at most. Considering a grid size of 10 m, this represents a high level of precision, providing sufficient reliability for practical maritime traffic control environments.

A noteworthy aspect of the results is the consistent accuracy achieved across vessels of various sizes and characteristics. For the largest vessel shown in Figure 4(d), despite its LOA of 286 m, the RE was only 5 m. This suggests that the grid-based approach can provide stable predictions regardless of vessel size. Similarly, the smallest vessel in Figure 4(c) also showed excellent accuracy, with an RE of only 4 m.

Another significant advantage of the grid-based approach is its quantitative consideration of the difference between the AIS antenna position and the actual anchor drop position. While the existing VTS system simply determines the center of the anchor circle based on the AIS antenna position, the proposed methodology calculates the actual anchor drop position using Equation (2) and uses this as the center of the

anchor circle. This significantly improved the accuracy of anchor circle prediction by enabling more precise identification of the center of vessel rotation.

The visualization results in Figure 4 clearly show how the actual movement patterns of vessels change over time. The trajectory of each vessel is represented by a color gradation, providing an intuitive view of position changes over time after anchoring. This suggests that the movement of anchored vessels, which was previously assumed to be a simple circular domain, may actually have more complex patterns. However, the study results show that despite these complex movement patterns, the proposed methodology can accurately predict the maximum range of vessel movement.

The relationship between vessel physical characteristics and anchor circle radius is also a notable finding. Comparing the data in Tables 2 and 3 confirms that the vessel size according to Equation (1) and anchor chain length according to Equation (5) directly influence the final anchor circle radius. For the vessels in Figures 4(a) and 4(d), the relatively large d_{stern} values (38 and 56 m, respectively) contributed significantly to the final anchor circle radius, demonstrating that detailed consideration of vessel physical characteristics is essential for accurate anchor circle determination.

The methodological feature of this study is the systematic approach shown in Equations (6) and (7). Particularly, the anchor circle radius calculation formula enables accurate prediction of the maximum movement range by considering both the total vessel length and anchor chain length. This formula has the advantage of allowing accurate anchor circle determination without complex calculations, while being simple yet effective.

The grid conversion process (Equation (7)) is another important methodological contribution. By converting continuous distance values into discrete grid units, implementation and visualization become easier, and consistent representation across various vessel sizes becomes possible. The maximum GNE of 1 shown in the experimental results demonstrates that this conversion process can provide practical benefits without significantly compromising accuracy.

Another important aspect of the proposed methodology is its immediate applicability in actual operational environments. The vessel specification information presented in Table 2 is data already collected in the current VTS system, eliminating the need for additional data collection infrastructure to implement the proposed methodology. This means that immediate application is possible simply by integrating the developed algorithm into the current system.

Accurate determination of anchor circles can contribute not only to maintaining safe distances between vessels but also to the early detection of abnormal movement, such as anchor dragging. While it is difficult to immediately detect when a vessel exceeds its actual movement range in the overestimated anchor circles of the current system, the proposed methodology enhances the possibility of early detection of abnormal situations through more accurate prediction of movement ranges. This is an important additional benefit from a maritime safety perspective.

5. Conclusion

This study proposes a grid-based anchor circle decision method that integrates vessel physical characteristics with AIS data to overcome the limitations of existing fixed-radius approaches in VTS systems. The developed method systematically incorporates vessel LOA, AIS antenna position, and anchor chain length to enable more accurate determination of actual vessel movement ranges during anchoring.

The main achievements include the establishment of a standardized grid-based framework that enables customized anchor circle decisions based on individual vessel characteristics, and experimental validation using actual vessel data from Busan Port anchorage.

Quantitative analysis revealed that existing VTS systems overestimate the required range by 1.7-2.1 times compared to the proposed method, which determines actual vessel movement ranges with significantly improved accuracy, achieving maximum RE of 9 m and GNE of 1. This contributes substantially to efficient anchorage operation and safe distance maintenance between vessels.

From an implementation perspective, the methodology demonstrates immediate practical applicability since current VTS systems already collect the necessary real-time information including vessel anchoring position, time, and heading angle. This enables automatic determination and display of accurate anchor circles upon vessel anchoring. However, the study has limitations including a small sample size, consideration of only single anchor operations, and testing under stable weather conditions without analyzing environmental factors such as wind and current effects.

Future research directions include developing comprehensive decision models incorporating weather conditions through machine learning techniques, evolving toward optimal anchoring position recommendation systems considering multi-vessel interactions, and creating dynamic anchor circle adjustment models that integrate environmental data. Such advances will provide core technologies for smart port implementation.

ACKNOWLEDGMENTS

This work has supported by Korea Institute of Marine Science & Technology Promotion (KIMST) funded by the Korea Coast Guard (RS2023-00238652, Integrated Satellite-based Applications Development for Korea Coast Guard) and the Ministry of Oceans and Fisheries (20210046 / RS-2021-KS211406, Development of marine satellite image analysis application technology).

REFERENCES

- [1] Xu, L., Huang, L., Zhao, X., Liu, J., Chen, J., Zhang, K., He, Y., 2025. Navigational decision-making method for wide inland waterways with traffic separation scheme navigation system. *Brodogradnja* 76(2), 76201. <https://doi.org/10.21278/brod76201>
- [2] Gao, J., Zhang, Y., 2024. Ship collision avoidance decision-making research in coastal waters considering uncertainty of target ships. *Brodogradnja* 75(2), 75203. <https://doi.org/10.21278/brod75203>
- [3] Zhang, W., Zhang, Y., 2023. Research on classification and navigational risk factors of intelligent ship. *Brodogradnja* 74(4), 105-128. <https://doi.org/10.21278/brod74406>
- [4] Praetorius, G., Hollnagel, E., Dahlman, J., 2015. Modelling Vessel Traffic Service to understand resilience in everyday operations. *Reliability Engineering & System Safety*, 141, 10-21. <https://doi.org/10.1016/j.ress.2015.03.020>
- [5] ESKI, Ö., Tavacioglu, L., 2024. A combined method for the evaluation of contributing factors to maritime dangerous goods transport accidents. *Brodogradnja* 75(4), 75408. <https://doi.org/10.21278/brod75408>
- [6] Fujii, Y., Tanaka, K., 1971. Traffic capacity. *The Journal of Navigation*, 24(4), 543-552. <https://doi.org/10.1017/S0373463300022384>
- [7] Goerlandt, F., Montewka, J., 2015. Maritime transportation risk analysis: review and analysis in light of some foundational issues. *Reliability Engineering & System Safety*, 138, 115-134. <https://doi.org/10.1016/j.ress.2015.01.025>
- [8] Zhang, W., Goerlandt, F., Kujala, P., Wang, Y., 2016. An advanced method for detecting possible near miss ship collisions from AIS data. *Ocean Engineering*, 124, 141-156. <https://doi.org/10.1016/j.oceaneng.2016.07.059>
- [9] Szlapczynski, R., Krata, P., Szlapczynska, J., 2018. Ship domain applied to determining distances for collision avoidance manoeuvres in give-way situations. *Ocean Engineering*, 165, 43-54. <https://doi.org/10.1016/j.oceaneng.2018.07.041>
- [10] Lu, Z., Kang, L., Gao, S., Meng, Q., 2018. Determination of minimum distance to obstacle avoidance in the Singapore strait. *Transportation Research Record*, 2672(11), 73-80. <https://doi.org/10.1177/0361198118794056>
- [11] Szlapczynski, R., Niksa-Rynkiewicz, T., 2018. A framework of a ship domain-based near-miss detection method using mamdani neuro-fuzzy classification. *Polish Maritime Research*, 25(s1), 14-21. <https://doi.org/10.2478/pomr-2018-0017>
- [12] Gao, X., Makino, H., 2017. Analysis of anchoring ships around coastal industrial complex in a natural disaster. *Journal of Loss Prevention in the Process Industries*, 50, 355-363. <https://doi.org/10.1016/j.jlp.2016.12.003>
- [13] Jingsong, Z., Zhaolin, W., Fengchen, W., 1993. Comments on ship domains. *The Journal of Navigation*, 46(3), 422-436. <https://doi.org/10.1017/S0373463300011875>
- [14] Dinh, G. H., Im, N. K., 2016. The combination of analytical and statistical method to define polygonal ship domain and reflect human experiences in estimating dangerous area. *International Journal of e-Navigation and Maritime Economy*, 4, 97-108. <https://doi.org/10.1016/j.enavi.2016.06.009>
- [15] Antunes, N., Ferreira, J. C., Pereira, J., Rosa, J., 2022. Grid-based vessel deviation from route identification with unsupervised learning. *Applied Sciences*, 12(21), 11112. <https://doi.org/10.3390/app12211112>

- [16] Sun, S., Guan, W., Wang, Y., 2024. Occupancy grid based environment sensing for MASS in complex waters. *Ocean Engineering*, 303, 117848. <https://doi.org/10.1016/j.oceaneng.2024.117848>
- [17] Liu, C., Guo, S., Feng, Y., Hong, F., Huang, H., Guo, Z., 2019. L-VTP: Long-term vessel trajectory prediction based on multi-source data analysis. *Sensors*, 19(20), 4365. <https://doi.org/10.3390/s19204365>
- [18] Guo, S., Liu, C., Guo, Z., Feng, Y., Hong, F., Huang, H., 2018. Trajectory prediction for ocean vessels base on k-order multivariate Markov chain. In *Proceedings of the 13th International Conference on Wireless Algorithms, Systems, and Applications*, June 20-22, Tianjin, China, 140-150. https://doi.org/10.1007/978-3-319-94268-1_12
- [19] Mandalis, P., Chondrodima, E., Kontoulis, Y., Pelekis, N., Theodoridis, Y., 2024. A transformer-based method for vessel traffic flow forecasting. *GeoInformatica*, 1-25. <https://doi.org/10.1007/s10707-024-00521-z>
- [20] Shin, G. H., Yang, H., 2025. Vessel trajectory prediction in harbors: A deep learning approach with maritime-based data preprocessing and Berthing Side Integration. *Ocean Engineering*, 316, 119908. <https://doi.org/10.1016/j.oceaneng.2024.119908>
- [21] Busan Regional Office of Oceans and Fisheries, 2024. Rules on Navigation of Busan Port, etc. *Notice No. 2024-24 of Busan Regional Office of Oceans and Fisheries*.
- [22] Lian, Y., Pan, Z., Zheng, J., Chen, W., Yim, S. C., 2025. Experimental investigation on mechanical behavior of damaged HMPE mooring ropes under service loads. *Marine Structures*, 101, 103760. <https://doi.org/10.1016/j.marstruc.2024.103760>
- [23] Amante, C. J., Eakins, B. W., 2016. Accuracy of interpolated bathymetry in digital elevation models. *Journal of Coastal Research*, Special Issue No. 76, 123–133. <https://doi.org/10.2112/SI76-011>
- [24] Eakins, B. W., Grothe, P. R., 2014. Challenges in building coastal digital elevation models. *Journal of Coastal Research*, 30(5), 942–953. <https://doi.org/10.2112/JCOASTRES-D-13-00192.1>
- [25] Tu, E., Zhang, G., Rachmawati, L., Rajabally, E., Huang, G. B., 2017. Exploiting AIS data for intelligent maritime navigation: A comprehensive survey from data to methodology. *IEEE Transactions on Intelligent Transportation Systems*, 19(5), 1559-1582. <https://doi.org/10.1109/TITS.2017.2724551>
- [26] Tetreault, B. J., 2005. Use of the automatic identification system (AIS) for maritime domain awareness (MDA). In *Proceedings of MTS/IEEE OCEANS*, September 18-23, Washington, D.C., United States, 1590-1594.
- [27] Korea Meteorological Administration (KMA), 2024. Weather Forecast Standards and Advisory/Warning Criteria.
- [28] Lian, Y., Zhang, Y., Xie, Y., Zheng, J., Chen, W., Chen, S. C., Yim, S. C., 2025. Effects of bedding-in loading history on mechanical behaviors of aramid HMPE and polyester mooring ropes. *Ocean Engineering*, 321, 120413. <https://doi.org/10.1016/j.oceaneng.2025.120413>
- [29] Lian, Y., Zhang, B., Zheng, J., Liu, H., Ma, G., Yim, S. C., Zhao, Y., 2022. An upper and lower bound method for evaluating residual strengths of polyester mooring ropes with artificial damage. *Ocean Engineering*, 262, 112243. <https://doi.org/10.1016/j.oceaneng.2022.112243>